Transcriptome Changes in Porcine Granulosa Cells in Response to Gossypol Cytotoxicity

Min-Wook Hong
Kangwon National University https://orcid.org/0000-0002-1603-7145
So-Young Choi
Kangwon National University
Hun Kim
Kangwon National University
Sung-Jin Lee (sjlee@kangwon.ac.kr)
Kangwon National University https://orcid.org/0000-0001-9348-8356

Research

Keywords: Gossypol, RNA-seq, Differentially expressed genes Porcine, Granulosa cells

Posted Date: February 25th, 2021

DOI: https://doi.org/10.21203/rs.3.rs-245034/v1

Transcriptome Changes in Porcine Granulosa Cells in Response to Gossypol Cytotoxicity

Min-Wook Hong, So-Young Choi, Hun Kim, Sung-Jin Lee*

College of Animal Life Sciences, Kangwon National University, Chuncheon, 24341, Republic of Korea

Min-Wook Hong email: winhonest@gmail.com

So-Young Choi email: csy0312@kangwon.ac.kr

Hun Kim email: hune1809@naver.com

* Corresponding author: Sung-Jin Lee

Email: sjlee@kangwon.ac.kr

Phone number: +82-10-5419-8905

Abstract

Background: Gossypol (GP) is a polyphenolic compound in cottonseed. In porcine, GP affects female reproduction and the respiratory system. The aim of this study was to identify differentially expressed genes in porcine granulosa cells (GCs) treated with GP (6.25 and 12.5 μM) for 72 h, *in vitro*.

Results: In GP-treated groups (6.25 and 12.5 μM), the expressions of a number of genes were found to be significantly changed. Gene ontology analysis indicated that the identified DEGs were primarily related to the mitotic cell cycle, chromosome, centromeric region and protein binding. Kyoto Encyclopedia of Genes and Genomes pathway analysis of the GP6.25 group revealed that pathways related to the cell cycle, oocyte meiosis, progesterone-mediated oocyte maturation and p53 signaling were the most changed, while that of the GP12.5 group revealed that pathways related to the PI3K-Akt signaling, focal adhesion, HIF-1 signaling, cell cycle and ECM-receptor interaction were the most changed. Genes associated with female reproductive function (*CDK1*, *CCNB1*, *CPEB1* and *MMP3*), cellular component organization (*BIRC5*, *CYP1A1*, *TGFβ3* and *COL1A2*) and oxidation-reduction processes (*PRDX6*, *MGST1* and *SOD3*) were confirmed to be differently expressed in GP-treated groups.

Conclusion: Our findings provide insight regarding changes in GC gene expression in porcine exposed to GP.

Keywords: Gossypol, RNA-seq, Differentially expressed genes Porcine, Granulosa cells

Introduction

Cottonseed and cottonseed meal (CM) are used as protein sources for livestock. While CM is most commonly used as feed for ruminants, its use has been increasing in poultry and monogastric animal species. However, both cottonseed and CM are known to contain a toxic substance, namely, gossypol (GP), which limits the use of CM as animal feed. GP (2,2-bi(8-formyl-1,6,7-trihydroxy-5-isopropyl-3-methylnaphthalene)) is a yellowish polyphenolic compound found in the roots, leaves, stems and seeds of the cotton plant genus Gossypium subspecies. It is known to affect male reproduction, inhibiting spermatogenesis and reducing spermatozoid motility and viability [1, 2], and the use of GP as a contraceptive agent in humans has been documented [3]. GP is absorbed into the body, and it does not decompose well and continues to accumulate. Absorbed GP appears to have a long half-life and has been detected in various organs and tissues, including plasma, heart, liver, kidney, muscle, testes and ovaries. In general, acute toxicity symptoms of GP in livestock include respiratory distress, impaired body weight gain, anorexia, weakness, apathy and death after several days [4-6]. In addition, certain clinical signs of GP poisoning have been attributed to reduced levels of antioxidants in tissues and increased reactive oxygen species (ROS) formation, resulting in lipid peroxidation [7, 8]. At high concentrations, GP has also been reported to impair energy production from oxidative metabolism by interfering with the mitochondrial electron transport chain and oxidative phosphorylation [9].

Ovarian follicles are composed of granulosa and theca cells, and oocytes surrounded by them. The growth of granulosa cells (GCs) and oocytes supports early follicle growth; in this process, GCs surround the oocytes and produce ovarian steroid hormones such as estrogen and progesterone [10, 11]. Ovarian steroids play important roles for the normal development and function of several organs, including the brain, uterus and mammary glands [12]. However, few studies have investigated the toxicity of GP using GCs, and among them, only changes in reproductive hormones or specific genes have been investigated [13-15].

In recent years, with development of the high-throughput technology capable of processing large amounts of data, and cost reduction of next-generation sequencing (NGS), sequence-based transcriptome analysis such as RNA sequencing (RNA-seq) is used not only in human but also in various animals and plants. RNA-seq has been shown to have considerable advantages such as examining transcriptome profile and differentiate between different transcriptional and splicing isoforms [16, 17]. Moreover, RNA-seq technology is known to be useful for analyzing

expression patterns of gene populations and understanding the regulatory networks of various metabolic pathways of the analyzed genes [18].

To our knowledge, no studies have used RNA-seq to identify how GP toxicity affects GCs in livestock. Especially, previous studies investigating the effects of GP toxicity, with the goal of identifying differences in gene expression, have not been conducted in porcine. Therefore, this study aims to systematically examine changes in gene expression as a result of GP treatment in porcine GCs using RNA-seq.

Methods

All experimental procedures were conducted in accordance with guidelines approved by the Institutional Animal Care and Use Committee of Kangwon National University, Chuncheon, Korea (KIACUC-18-061).

Isolation and GCs primary culture. Prepubertal gilt ovaries were obtained from a local slaughterhouse and transported to the laboratory within 2 h of isolation in a vacuum thermos flask in 0.9% sterile physiological saline at 37°C. Follicular fluid and GCs were aspirated from follicles with a diameter of 3–6 mm that contained clear follicular fluid using 10 ml syringe with 18-gauge needle. The GCs were then transferred to a 15-ml centrifuge tube and centrifuged at 500 × g for 5 min for precipitation. Precipitated cells were resuspended with ammonium chloride (NH_4Cl) at 37°C for 1 min to remove red blood cells. The cells were then washed twice with phosphate-buffered saline (PBS) containing 1% penicillin-streptomycin solution. GCs were cultured in DMEM/F12 (Gibco, Carlsbad, CA, USA) medium supplemented with 10% FBS (Gibco) and 1% penicillin-streptomycin solution in a humidified incubator with 5% CO_2 at 37°C for 3 days. When a complete monolayer had formed in the primary culture, the GCs were washed with PBS, trypsinised and harvested for additional experiments.

Subculture and GP treatments. Stock solutions of GP were prepared by first dissolving GP in DMSO at a 10mM concentration and it was stored in aliquots at −20°C until further use. The stock solution was then diluted to concentrations of 0.625, 1.25 and 2.5 mM in DMSO before start of experiments. For experiments, the diluted GP was further diluted (1 in 100) when added to the cell culture medium. The obtained cells from primary culture

were subcultured into wells or dishes in suitable amount for each experiment with 1×10^6 cells/dish in 100 mm culture dishes (SPL Life science, Pocheon, Korea) for RNA-seq, 1×10^5 cells/well in 6-well culture plates (SPL Life science) for qRT-PCR and Western blot analysis and 0.5×10^4 cells/well in 96-well culture plates (SPL Life science) for cellular proliferation assays. All culture plates and dishes were incubated at 5% CO_2 at 37°C. After seeding the cells for 24 h, to study the cytotoxic effects of GP in GCs, GP was added to the medium at final concentrations of 6.25, 12.5 and 25 μM and the cells were incubated for 72 h. The GP untreated group (Ctrl) was incubated with only DMSO at the same concentrations as the GP treatment groups to ensure the accuracy of the experimental design. The experiment was repeated three times with identical conditions to provide three biological replicates for each time point and treatment.

Measurement of cell proliferation. GCs (0.5×10^4 cells/well) were seeded with 200 μL culture medium in 96 well plates. After a culture period of 24 h, the cells were treated with various final concentrations of GP (6.25 to 25 μM) for 72 h, while DMSO-treated cells without GP treatment served as the Ctrl group. The proliferation of GCs was measured at 570 nm using a microplate reader with the CellTiter 96 Non-Radioactive Cell Proliferation Assay (Promega, Madison, WI, USA) according to the manufacturer's instructions.

RNA extraction, library construction and sequencing analysis. After GP treatment, total RNA was extracted from the GCs using Trizol reagents (Invitrogen, Carlsbad, CA, USA). RNA extraction was performed in duplicate for each sample. The obtained total RNA was assessed using the Agilent 2100 Bioanalyzer (Agilent technologies, CA, USA). The Illumina TruSeq Stranded mRNA Sample Preparation kit (Illumina, San Diego, USA) was used for preparing mRNA sequencing library from the isolated total RNA. All libraries were quantified by qPCR using a CFX96 Real-Time PCR Detection System (Bio-Rad, Hercules, CA, USA) and sequenced with a paired-end 75 bp plus single 8 bp index reads using a NextSeq 500 sequencers (Illumina). Potentially existing sequencing adapters and low-quality bases (5' and 3' ends) in the raw reads were trimmed by Skewer software [19]. The cleaned high-quality reads after trimming the low-quality bases and sequencing adapters were mapped to the reference genome by STAR software [20]. The calculation of Q30, GC content and sequence duplication levels were based on the clean reads using by FastQC (http://www.bioinformatics.babraham.ac.uk/projects/fastqc/).

Identification of DEGs. The mapped reads for gene expression values were assembled with Cufflinks following the porcine reference genome (*susScr11*) annotation [21]. The gene annotation of the reference genome from the UCSC genome (https://genome.ucsc.edu) in GTF format was used as a gene model and the expression values were calculated in the fragments per kilobase of transcripts per million mapped reads (FPKM) unit. The differentially expressed genes (DEGs) between the two selected biological conditions were analyzed by Codify software in Cufflinks package [22]. To compare the expression profiles among the samples, the normalized expression values of the selected few hundred DEGs were unsupervised clustered by in-house R scripts.

GO enrichment and KEGG pathway enrichment analysis. To gain insight into the biological and functional roles of the DEGs, gene set overlapping between the analyzed DEGs and functional categorized genes, including biological processes of Gene Ontology (GO), Kyoto Encyclopedia of Genes and Genomes (KEGG, www.kegg.jp/kegg/kegg1.html) pathways and other functional gene sets by g:Profiler (https://biit.cs.ut.ee/gprofiler), was performed [23]. A corrected p-value of 0.05 was set as the threshold to identify significantly different pathways [24] and p-values were adjusted using the Benjamini-Hochberg method [25].

Quantitative RT-PCR. cDNA was reverse transcribed from 500 ng of total RNA using iScript cDNA synthesis kit (Bio-Rad), while qRT-PCR analyses were performed using an ABI 7500 Real Time PCR System (Applied Biosystems, CA, USA). PCR was conducted in a 20 µl reaction volume with PowerUP SYBR Green Master Mix (Thermo Fisher Scientific, Waltham, MA, USA) and 0.4 pmol of specific primer pairs (Supplementary Table 1). The general qRT-PCR reaction conditions were as follows (except *MMP3* and *SOD3* genes): 2 min at 50°C, 2 min at 95°C, followed by 45 cycles of 15 s at 95°C, 1min at 60°C. The qRT-PCR conditions of the *MMP3* gene were as follows: 2 min at 50°C, 10 min at 95°C, followed by 45 cycles of 30 s at 95°C, 30 s at 59°C and 30 s at 72°C, with a final extension of 10 min at 72°C. The qRT-PCR conditions for the *SOD3* gene were as follows: 2 min at 50°C, 10 min at 95°C, followed by 50 cycles of 30 s at 95°C, 30 s at 59°C and 30 s at 72°C, with a final extension of 10 min at 72°C. The standard curve of the *β-actin* gene in porcine GCs was used as the reference to normalize the mRNA expression of the gene of interest. The relative expression of the genes was calculated using

the $2^{-\Delta\Delta Ct}$ method. Three separate experiments were performed on different cultures and each sample was assayed in triplicate.

Western blot analysis. Protein lysates isolated from GCs were used for Western blot using the PRO-PREP Protein Extraction Solution (Intron Biotechnology, Seongnam, Korea) according to manufacturer's procedure. Protein concentrations were determined using a Pierce BCA Protein Assay Kit (Thermo Fisher Scientific). Samples containing 10 µg protein were boiled in Laemmli buffer and resolved on 12% Tris-glycine polyacrylamide gels and then transferred to polyvinylidene fluoride (PVDF) membranes (Millipore Corporation, Bedford, MA, USA). The membranes were blocked in 5% skim milk and incubated with primary antibodies as follows: anti-MGST1 (MyBioSource, San Diego, CA), 1:500; anti-PRDX6 (MyBioSource), 1:1000; CCNB1 (Aviva Systems Biology, San Diego, CA, USA), 1:1000; MMP3 (Biorbyt, Cambridge, UK), 1:250; β-actin (Biorbyt), 1:500 for 2 h at RT. The membranes were washed in TBST and then incubated with secondary antibody (mouse anti-rabbit IgG-HRP, Santa Cruz, CA, USA; 1:2500) for 1 h at RT. Immunoreactive bands were detected using the Pierce ECL Plus Western Blotting Substrate (Thermo Fisher Scientific) in conjunction with ImageQuant LAS 500 imager system (GE Healthcare, Little Chalfont, UK). Relative sample intensities were computed by scanning and quantifying the immunoblot data using ImageJ software (National Institutes of Health, Bethesda, MD, USA) [26]. Each Western blot experiment was performed three times and representative image results are shown. Semiquantitative results are reported as the mean ± SEM.

Statistical analysis. Differences between the Ctrl and GP-treated groups were statistically determined using one-way analysis of variance. Results are presented as mean ± SEM of at least three separate experiments performed on different cultures. All statistical analyses were performed using SAS software ver. 9.4 (SAS institute Inc., NC, USA). Results were considered statistically significant at $p < 0.05$. Frequency distribution graphs were plotted using GraphPad Prism ver. 7.0 (GraphPad software Inc., San Diego, CA, USA).

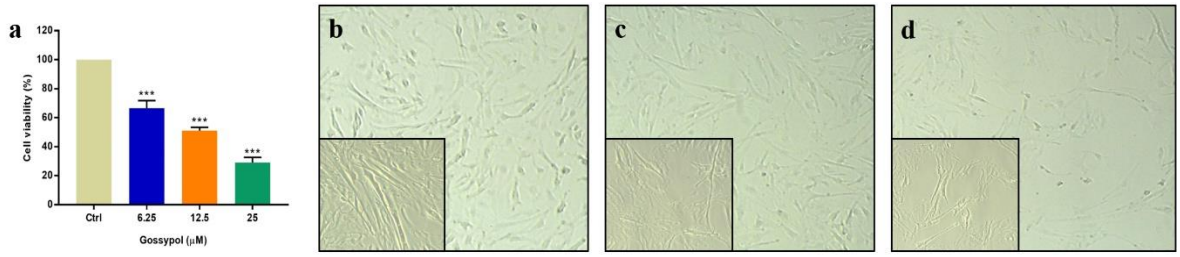

Figure 1. Effect of GP on the viability of porcine GCs *in vitro*. Porcine GCs were cultured with 0, 6.25, 12.5 and 25 μM GP for 72 h. (a) GC viability at different concentrations (6.25–25 μM) of GP. Data are expressed as mean ± SEM (n = 3) ***p < 0.001. (b)–(d) present the morphology of cultured GCs treated with GP. Large pictures were captured at 40× magnification, while small pictures were captured at 100× magnification. (b) GCs cultured in 0 μM GP (non-treated). (c) GCs cultured in 6.25 μM GP. (d) GCs cultured in 12.5 μM GP. GP: gossypol, GCs: granulosa cells, Ctrl: GP untreated in GCs.

Results

GP exposure affected the number of viable porcine GCs. To evaluate changes in cellular viability as a result of GP treatment, cell viability assays of GCs were performed after GP treatment at different concentrations for 72 h (Figure 1a). Our results showed that the viability of the GCs significantly decreased ($p < 0.001$) with GP treatment (6.25 to 25 μM), compared with Ctrl. GCs cultured with 12.5 μM GP (GP12.5) showed cellular viability levels that were close to the IC50 concentration (i.e., the half maximal inhibitory concentration) at 51.2%. Based on the above results, we observed the cell morphology of the Ctrl, GP6.25 (GP 6.25 μM treated GCs) and GP12.5 using a microscope (Figure 1, b to d).

Overview of sequencing data using RNA-seq analysis. All three groups, GP6.25, GP12.5 and Ctrl groups, consisted of two cDNA libraries each. Mapped reads and annotation showed that the three libraries were of high quality, with a total of 20,526,910, 17,897,687 and 20,352,139 sequences that were matched, respectively (Table 1). The reads were obtained for about 88.33% of the porcine reference genome (*sus scrofa*) in NCBI. In addition, the Q30 range was determined to be from 89.5% to 92.1%. These finding suggests that the library quality for each group was good and suitable for analysis. The results of the hierarchical clustering of DEGs between the three groups showed a clear discrimination which is presented as a heat map in Figure 2a. The distribution of FPKM for all the samples were indicated as similar expression level, and most of the mRNAs detected in the RNA-seq analysis were also found to be protein-coding genes. (Figure 2b).

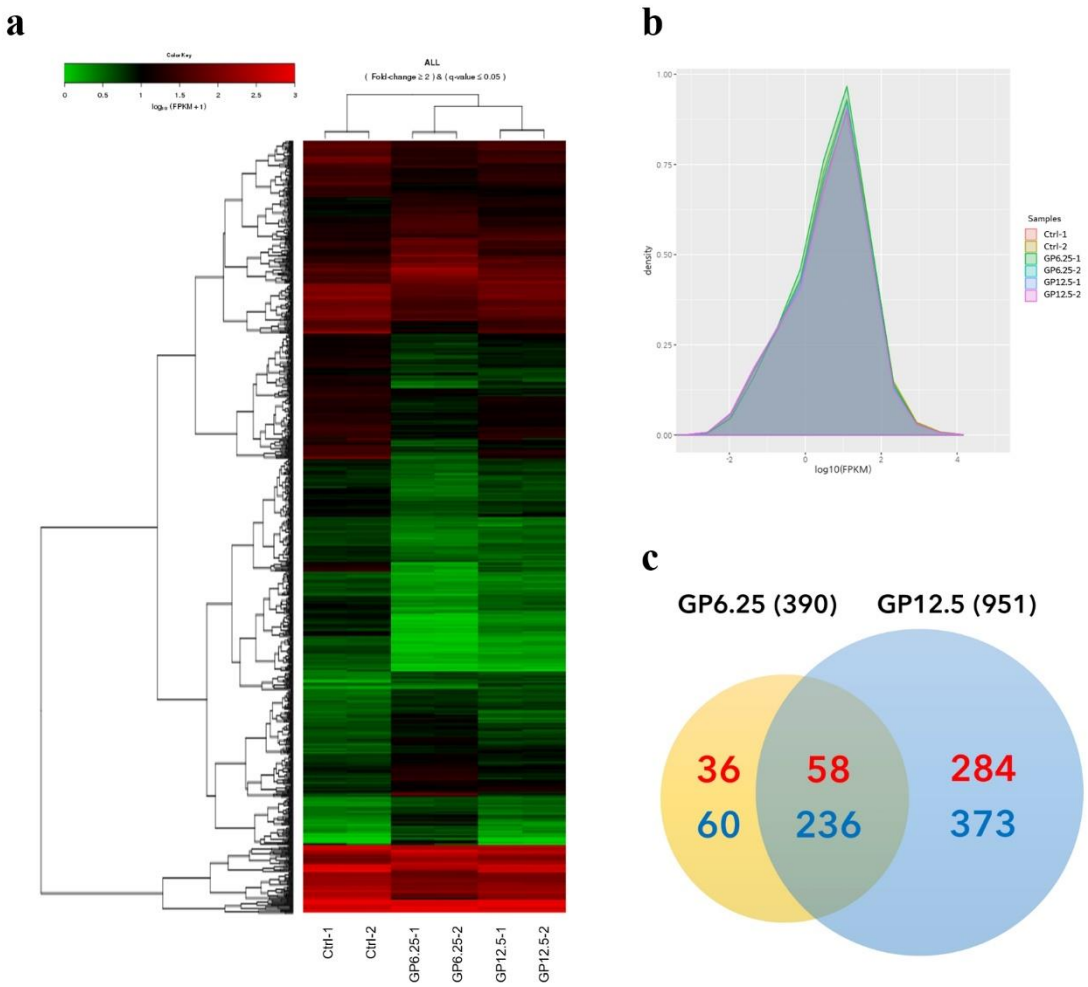

Figure 2. Summary of RNA-seq mapping data. (a) Comparative expression of selected transcriptomes across the GP-treated and Ctrl groups. Heatmap for the expression values in log10 (FPKM) units of the selected DEGs. Red indicates upregulated, while green indicated downregulated gene expression ($p < 0.05$). (b) Density plot for log10 (FPKM) values to compare gene expression between each sample. (c) Venn diagram showing the number of differently expressed genes between the GP6.25 and GP12.5 groups ($p < 0.05$). Red colour: upregulated, Blue colour: downregulated, Ctrl: GP untreated GCs, GP6.25: GP 6.25 µM treated GCs, GP12.5: GP 12.5 µM treated GCs, GP: gossypol, GCs: granulosa cells

Differential gene expression of GCs by GP exposure using RNA-seq analysis. The number of found genes in each library group was 14,344, 14,294 and 14,482, respectively (Table 1). Among them, a total of 390, 951 significantly different genes were obtained from the GP6.25 and GP12.5 groups with the conditions of $p < 0.05$, FDR < 0.05 and $|FC| \geq 2$ (Figure 2c). In the GP6.25 group, compared with the Ctrl group, there were 94 upregulated DEGs and 296 downregulated DEGs, while in the GP12.5 group, there were 342 upregulated DEGs

and 609 downregulated DEGs. A total of 294 genes were identified, including 58 upregulated and 236 downregulated genes in intersection portion of both concentrations (IPC). Table 2 shows the most upregulated and downregulated genes overlapping with the GP6.25 and GP12.5 groups.

Table 1. Summary statistics of RNA-sequencing data obtained from GP-treated (6.25 and 12.5 µM) and untreated porcine GCs.

	Ctrl	**GP 6.25**	**GP 12.5**
Total reads	20,529,934	17,898,643	20,353,291
Mapped reads	20,526,910	17,897,687	20,352,139
Yield (Mb)	3,119	2,720	3,092
Q30	91.9	89.5	92.1
Mapping rate (%)	89.83	84.50	90.65
Unique mapped (%)	17,843,415 (86.93)	14,844,050 (82.94)	17,995,481 (88.42)
Multiple mapped (%)	597,953 (2.91)	405,462 (2.27)	450,752 (2.21)
Detected genes number	14,344	14,294	14,482

GCs: granulosa cells, Ctrl: GP untreated GCs, GP6.25: GP 6.25 µM treated GCs, GP12.5: GP 12.5 µM treated GCs

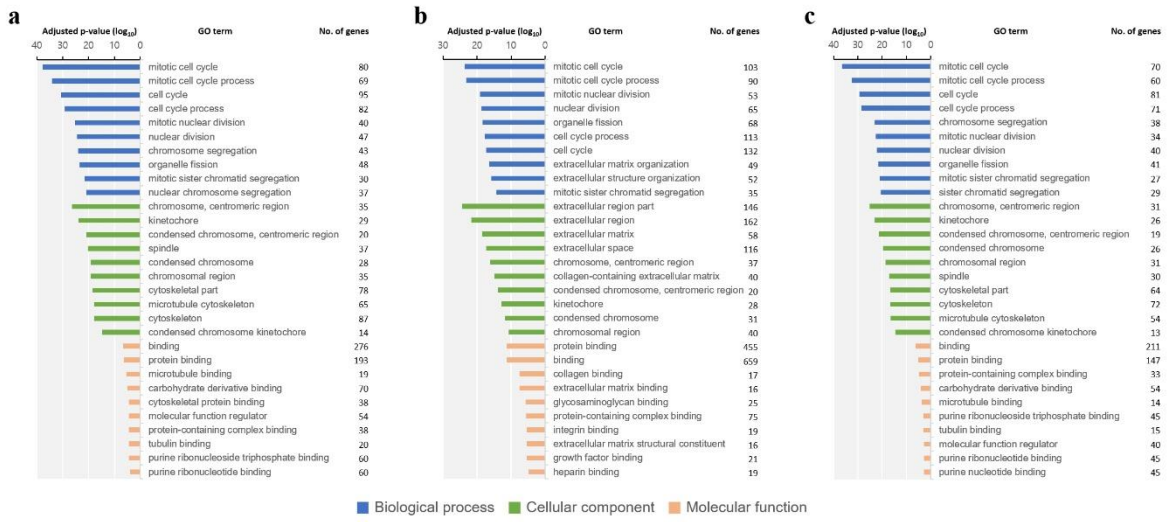

Figure 3. GO functional analysis of DEGs. GO term enrichment analysis results based on the different GP treatments were retrieved and compared with the Ctrl group using g:Profiler (https://biit.cs.ut.ee/gprofiler). The 10 most significantly ($p < 0.05$) enriched GO terms related to biological processes, cellular components and molecular functions are sown. All adjusted statistically significant values of the terms were −log10 converted. (a) GO term enrichment result of the DEGs in the GP6.25 group. (b) GO term enrichment result of the DEGs in the GP12.5 group. (c) GO term enrichment result of the DEGs in IPC group. GO: gene ontology, GP: gossypol, Ctrl: GP untreated GCs, GP6.25: GP 6.25 μM treated GCs, GP12.5: GP 12.5 μM treated GCs, IPC: intersection portion of both concentrations, GO: gene ontology, DEGs: differentially expressed genes

Functional classification of the top 30 GO terms for all DEGs of three group (GP6.25, GP12.5, IPC) is shown in Figure 3. In the biological process category, the GO terms found to be enriched in the DEGs were those related to 'mitotic cell cycle' and 'mitotic cell cycle process' for all groups. In the cellular component category, the enriched GO terms of interest included 'chromosome, centromeric region' and 'kinetochore' in the GP6.25 group and IPC group. However, the GO terms found to be the most enriched in the GP12.5 group were 'extracellular region part', 'extracellular region' and 'extracellular matrix'. In the molecular function category, the GO terms found to be enriched in the DEGs were centered on 'binding' and 'protein binding' for all groups. Each of the 170, 423 and 127 DEGs were then assigned to KEGG annotations in the GP6.25, GP12.5 and IPC groups. Our results indicated that 8, 30 and 8 enriched pathways were significantly changed ($p < 0.05$) in each group, respectively (Figure 4). The GP6.25 and IPC groups revealed that eight pathways including cell cycle, oocyte meiosis, progesterone-mediated oocyte maturation and p53 signaling pathways, were the most changed. The GP12.5 group was revealed that 30 pathways including PI3K-Akt signaling pathway, focal adhesion, HIF-1 signaling pathway, cell cycle and ECM-receptor interaction, were the most changed.

Table 2. Top 10 upregulated and downregulated genes in porcine GCs treated different concentration (6.25 and 12.5 μM) of GP compared with Ctrl.

Genes	Description	Log2 fold change		P-value	
		GP6.25	GP12.5	GP6.25	GP12.5
UP					
SLC2A5	Solute carrier family 2 member 5	1.232	4.250	0.00005	0.00005
SLC16A3	Solute carrier family 16 member 3	1.385	3.279	0.0004	0.00005
MMP3	Interstitial collagenase 18 kDa interstitial collagenase	2.896	3.279	0.00005	0.00005
SCD	Acyl-CoA desaturase	1.113	3.205	0.00005	0.00005
PPP1R3C	Protein phosphatase 1 regulatory subunit 3C	2.129	2.869	0.00005	0.00005
IL1RL1	Interleukin 1 receptor like 1	1.276	2.815	0.00005	0.00005
GPNMB	Transmembrane glycoprotein NMB precursor	1.710	2.740	0.00005	0.00005
SNTB1	Syntrophin beta 1	1.356	2.566	0.00005	0.00005
ENSSSCG00000027013	-	1.565	2.400	0.00005	0.00005
TFRC	Transferrin receptor protein 1	1.724	2.314	0.00005	0.00005
DOWN					
TOP2A	DNA topoisomerase 2-alpha	−2.442	−8.242	0.00005	0.00255
ENSSSCG00000002849	-	−2.731	−7.591	0.00005	0.0108
DLGAP5	DLG associated protein 5	−2.972	−6.474	0.00005	0.0001
ASPM	Abnormal spindle microtubule assembly	−4.055	−6.183	0.00005	0.00005
PBK	Lymphokine-activated killer T-cell-originated protein kinase	−1.604	−6.075	0.00005	0.00025

CCNB3	Cyclin B3	−2.915	−6.070	0.00005	0.0002
CCNB1	G2/mitotic-specific cyclin-B1	−3.370	−5.934	0.00005	0.00005
UBE2C	Ubiquitin conjugating enzyme E2 C	−2.957	−5.859	0.00005	0.00005
CCNB2	G2/mitotic-specific cyclin-B2	−2.840	−5.793	0.00005	0.00005
CDCA8	Cell division cycle associated 8	−2.814	−5.727	0.00005	0.0001

GCs: granulosa cells, GP: gossypol, Ctrl: GP untreated GCs, GP6.25: GP 6.25 μM treated GCs, GP12.5: GP 12.5 μM treated GCs

Validation of selected genes by qRT-PCR. Based on sequencing data and functional analysis, 11 genes of interest, including those associated with female reproductive functions (*CDK1*, *CCNB1*, *CPEB1* and *MMP3*), cellular component organisation (*BIRC5*, *CYP1A1*, *TGFβ3* and *COL1A2*) and oxidation-reduction process (*PRDX6*, *MGST1* and *SOD3*) were selected for validated by qRT-PCR. As shown in Figure 5, five genes (*CYP1A1*, *CPEB1*, *MMP3*, *PRDX6* and *MGST1*) were found to be significantly upregulated, and six genes (*CDK1*, *CCNB1*, *BIRC5*, *TGFβ3*, *COL1A2* and *SOD3*) were significantly downregulated in both groups treated with GP (GP6.25, GP12.5). these results were consistent with those obtained from RNA-seq. However, three genes (*CYP1A1*, *PRDX6* and *SOD3*) were not found to be significantly changed in the GP6.25 group. Overall, our results indicated that RNA-seq generated a reliable dataset for the transcriptome analysis of GP-treated GCs.

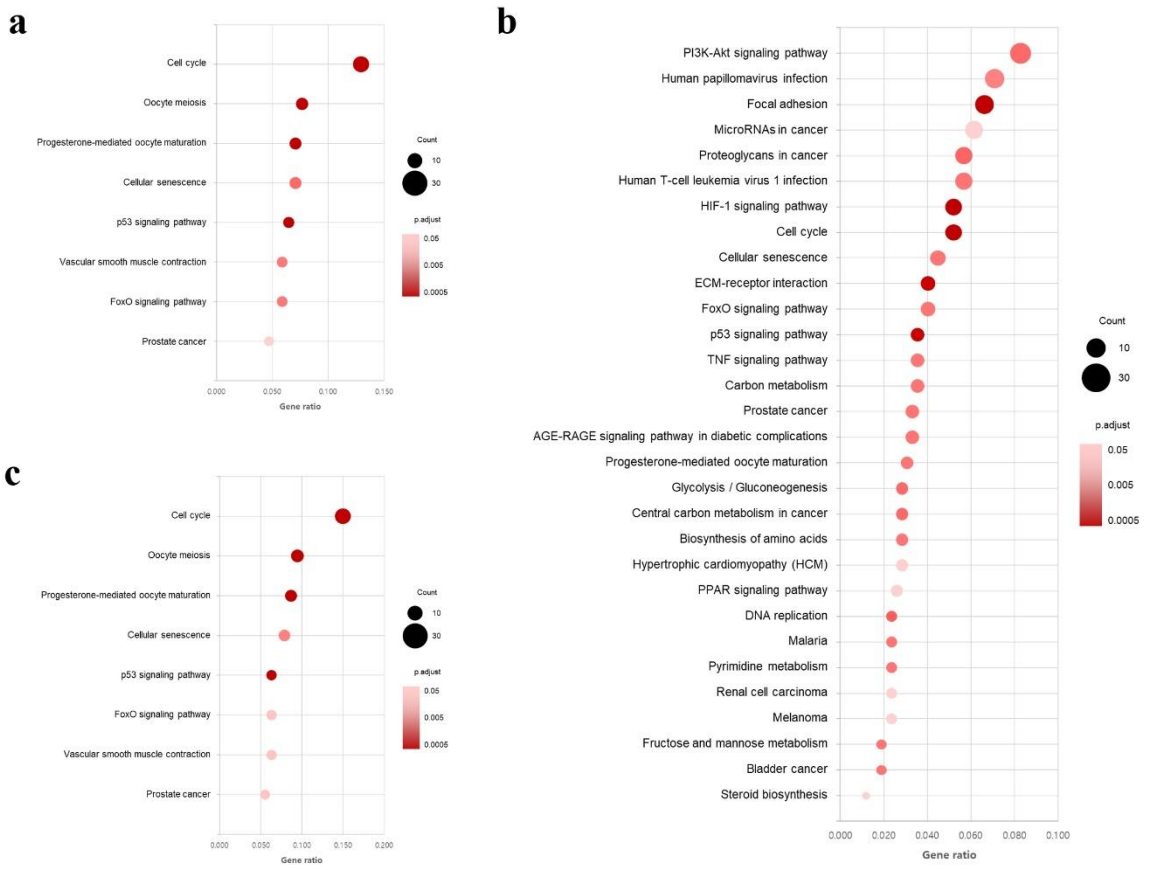

Figure 4. A scatter plot of the significantly enriched KEGG pathways ($p < 0.05$, www.kegg.jp/kegg/kegg1.html) of the DEGs based on transcriptome sequencing analysis of each GP-treated group compared with the Ctrl group. The y-axis represents the name of the pathway, while the x-axis represents the gene ratio. Dot size represents the number of genes and the colour indicated the p-value. (a) Enriched KEGG pathways of the DEGs in the GP6.25 group. (b) Enriched KEGG pathways of the DEGs in the GP12.5 group. (c) Enriched KEGG pathways of the DEGs in the IPC group. KEGG: Kyoto encyclopaedia of genes and genomes, DEGs: differentially expressed genes, GP6.25: GP 6.25 µM treated GCs, GP12.5: GP 12.5 µM treated GCs, IPC: intersection portion of both concentrations

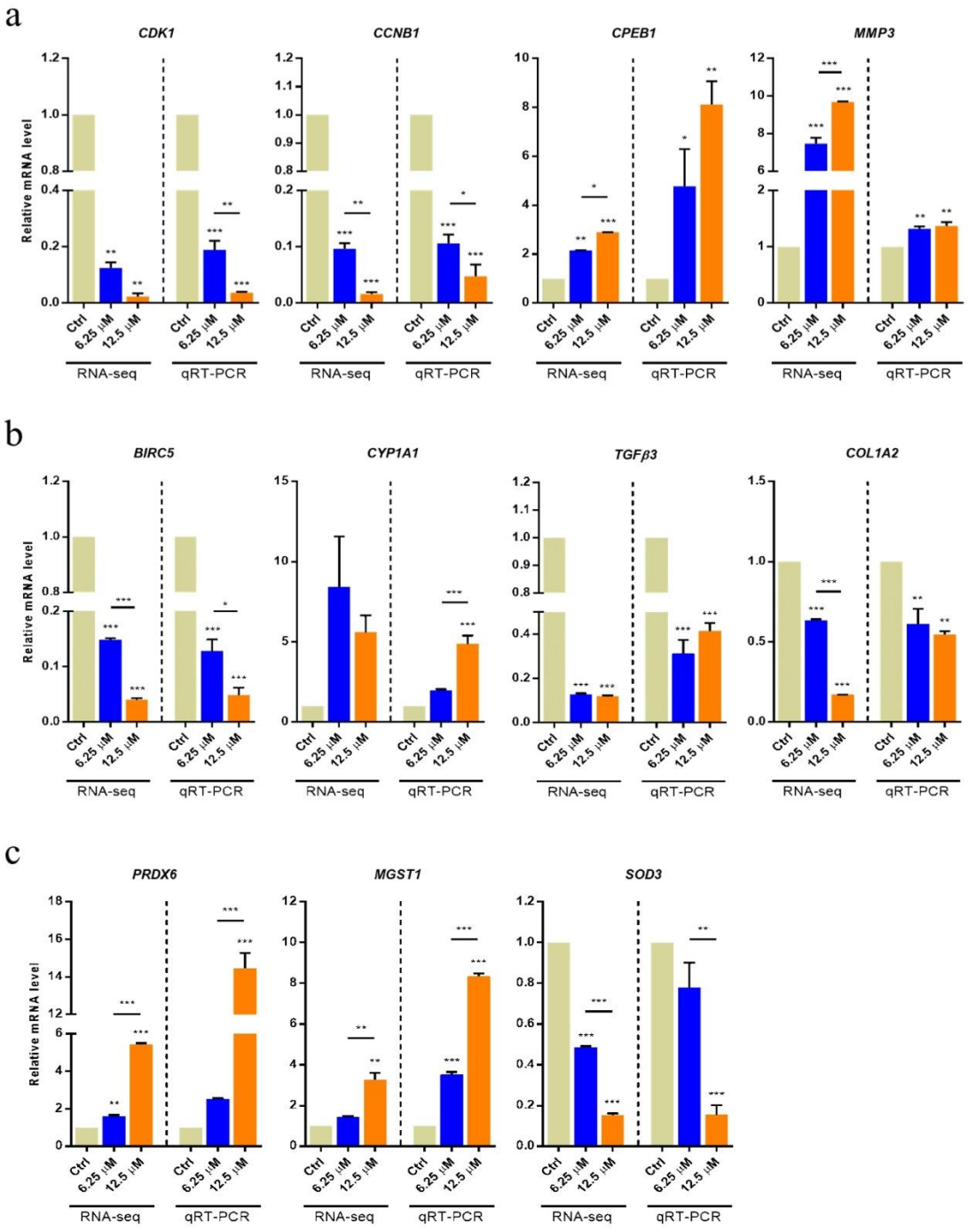

Figure 5. Quantification of the mRNA profile of GP-treated GCs (6.25 and 12.5 µM) using RNA-seq and qRT-PCR. GCs incubated with each GP concentration for 72 h. GP exposure affected the mRNA abundance of certain genes in the cells. (a) Cellular component organisation related genes (*BIRC5*, *CYP1A1*, *COL1A2* and *TGFβ3*) were measured and presented. (b) The female reproductive functions related genes (*CDK1*, *CCNB1*, *CPEB1* and *MMP3*) measured and presented. (c) Oxidation-reduction process related genes (*PRDX6*, *MGST1* and *SOD3*) were measured and presented. The mRNA levels of all genes were normalised to the porcine *β-actin* gene. Results are presented as mean ± SEM. All experiments were repeated at least three times. Ctrl: GP untreated GCs, GP: gossypol, GCs: granulosa cells, *p < 0.05; **p < 0.01; ***p < 0.001.

GP cytotoxicity induced various changes in GCs protein expression. Based on the mRNA expression results of qRT-PCR and RNA-seq, we selected four proteins for further Western blot analysis. The expression of proteins related to female reproductive function (CCNB1), cellular component organization (MMP3) and oxidative-reduction process (MGST1, PRDX6) are shown in Figure 6. In our results, the expression levels of three proteins significantly changed (increased or decreased) according to the difference of GP concentration, with the exception of the MGST1 protein. The expression of MGST1 protein was not significant, but an upregulated pattern was identified.

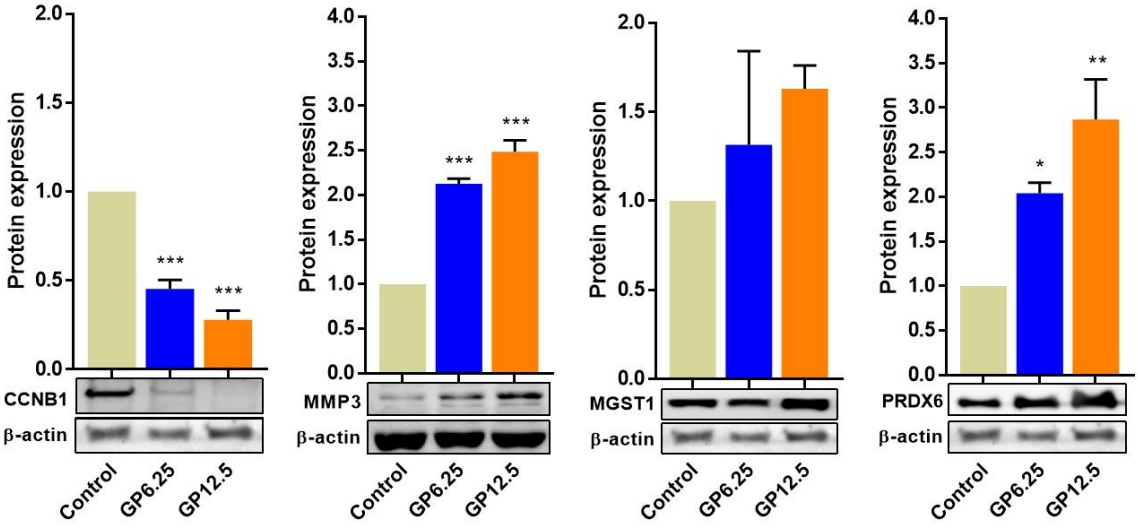

Figure 6. Western blot analysis of CCNB1, MMP3, MGST1 and PRDX6 proteins with different concentration of GP (6.25 and 12.5 μM) in porcine GCs. The protein levels were normalised to β-actin. Data are expressed as the mean ± SEM. All experiments were repeated at least three times. Full-length images for above cropped images are presented in Supplementary Fig. 1. Ctrl: GP untreated GCs, GP: gossypol, GCs: granulosa cells, *: $p < 0.05$, **: $p < 0.01$, ***: $p < 0.001$

Discussion

In recent years, RNA-seq, as a method for the sequence-based analysis of transcriptomes, has become a useful tool for analyzing gene expression patterns with high-throughput NGS technology. In addition, RNA-seq allows for the analysis of complex whole eukaryotic transcriptomes with higher reproducibility, wider dynamic range,

less bias and lower frequency of false positive signals compared with traditional cDNA microarray technologies [27]. An earlier study has reported that the Pearson correlation between RNA-seq and qRT-PCR could reach > 0.9 [28], suggesting that RNA-seq is an advanced technology that is reliable and reproducible. In addition, several studies using RNA-seq have been conducted on the porcine transcriptome such as the effects of ageing or various antioxidants in GCs [29-31]. However, to date, there exist limited studies that have investigated the toxic effects of GP in porcine, and the majority of these studies have focused on differences in internal organ size and changes in reproductive hormones [6, 32]. As such, the studies of gene effects on GCs by GP toxicity are currently almost unknown. Therefore, in this study, we investigated the transcriptome profile of the porcine GCs using RNA-seq, with the aim of identifying candidate genes for major functional changes caused by GP cytotoxicity.

Previous studies have shown that cellular proliferation is affected by GP toxicity. Indeed, GP has been shown to inhibit cell growth in a dose-dependent manner in various species, including human. The majority of the studies evaluating the toxic effects of GP at the cellular level have been performed on cancer cells, including those of leukaemia [33], prostate cancer [34], breast cancer [35], ovarian cancer [36], carcinoma [37] and other malignancies [38], with the focus of preventing cancer metastasis. As a result, it has been reported that the proliferation of cancer cells is inhibited by GP toxicity. However, unlike cancer cells, some studies using primary cells have shown a different pattern of cell growth by GP toxicity. Lin et al. [14] reported that GP at 10, 50 and 150 μg/ml significantly decreased the number of bovine oocytes undergoing cumulus expansion cultured at 24 h, by 15%, 50% and 80%, respectively. In another study, however, cellular proliferation was shown to be significantly increased by GP at 5 and 25 μg/ml in porcine GCs cultured for 44 h [39]. In this study, we found that the number of viable cells was dramatically decreased a dose-dependent manner in GP-treated porcine GCs. A possible reason for the discrepancy between the results of the present study and those from previous studies using primary cells may be related to differences in the culture period. However, Hsiao et al. [40] reported that the population of apoptotic cells increased significantly with increasing GP dose, and the cells were more likely to enter late apoptosis and undergo cell arrest compared with the control group. Collectively, our results suggested that the inhibition of proliferation by GP toxicity may occur after exposure to GP for a sufficient period of time.

In females, granulosa and theca cells, and oocytes are the constituents of mammalian ovarian follicles. GCs play a complex and central role in the development of the ovarian follicle During this process, GCs surround and nurse the oocyte, supporting its maturation. In this study, we identified DEGs from an RNA-seq library of porcine GCs

treated with two GP concentrations (6.25 and 12.5 μM). These DEGs were then divided into three groups (GP6.25, GP12.5 and IPC), and we investigated the differences in gene expression caused by GP toxicity through GO and KEGG pathway analysis. We have found that identified DEGs are associated with processes related to cellular component organisation, oxidation-reduction and female reproductive functions. From these results, we selected 11 genes to investigate differences in mRNA and protein expression as a result of GP exposure.

Meiotic progression and oocyte maturation are regulated by activity of the universal cell cycle regulator called the maturation-promoting factor (MPF). In addition, MPF is important for the precise regulation of mitosis and enables chromatin condensation and alignment through the histone phosphorylation regulation. As such, MPF, which plays an important role in the cell cycle, is a heterodimer mainly composed of a regulatory subunit, cyclin B (CCNB) and a catalytic subunit, cyclin-dependent kinase 1 (CDK1) [41, 42]. Adhikari et al. [43] reported that the *CDK1* gene is necessary to promote the resumption of meiosis. Jiang et al. [44] reported that cyclin and CDK accelerate cell cycle progression, whereas CDK inhibitors slow the progression. CCNB1 is known as a major protein involved in the regulation of oocyte maturation in mammals. The synthesis of CCNB1 is necessary for germinal vesicle breakdown (GVBD) induction in the second meiosis [45, 46]. Stanley et al. [47] reported that the levels of cyclin A, B1 and CDK1 were reduced by hexavalent chromium in rat GCs, delaying cell entry and progression through the G2-M phase. In the present study, the mRNA expression of *CDK1* and *CCNB1* was decreased in a dose-dependent manner in GP-treated GCs, as observed from both RNA-seq and qRT-PCR. We found that protein expression of CCNB1 also decreased in dose-dependently. These results suggest that GP indirectly inhibits the maturation and development of oocytes by delaying cell cycle progression by reducing the levels of *CDK1* and *CCNB1* in porcine GCs.

Translational activation and polyadenylation of cell cycle regulators including cyclins and CDK, are found primarily in the 3'-UTR of the mRNAs; the cytoplasmic polyadenylation element (CPE) is located in these sequences [48]. The CPE binds to the CPE-binding protein 1 (CPEB1), the CPEB1 is involved in translational activity or inhibition, according to the phosphorylation state [49]. In oocytes, the non-phosphorylated CPEB1 protein is known to interact with Maskin and Pumilio proteins, which are involved in translational repression [50, 51]. In previous studies of various species, including human, CPEB has been reported to be involved in both the inhibition and stimulation of *CCNB1* mRNA. In this regard, Nakahata et al. [51] reported that the overexpression of Pumilio in *Xenopus* oocytes leads to inhibition of *CCNB1* levels. Taken together, the phosphorylation of CPEB1

suggests that it may be involved in the regulation of CCNB1 activity. In our results, the mRNA expression of *CPEB1* was upregulated and that of *CCNB1* was downregulated. We have not been able to identify exactly how GP acts on the phosphorylation of CPEB1. However, our results suggested that Pumilio bound to the *CPEB1* gene likely regulated the levels of CCNB1. As a result, GP is involved in the expression of *CPEB1* and *CCNB1* genes in GCs; thus, it seems to be affecting the growth and maturation of oocytes.

In general, the extracellular matrix (ECM) is a natural substrate that supports the function of cells such as intercellular communication, adhesion, migration and proliferation. In particular, it affects cell morphology, follicle development, aggregation, communication and steroidogenesis in the ovary. ECM metabolism, which causes periodic changes throughout the reproductive cycle, is caused by the action of certain types of proteins known as the matrix metalloproteinases (MMPs). MMPs are enzymes that degrade ECM proteins throughout the body to facilitate tissue remodelling [52]. Many studies have shown that MMPs play an important role in follicle development, ovulation, luteinization and luteolysis associated with follicular ECM alterations [53, 54]. Zhu et al. [55] reported that the gene expression of *MMP1*, *MMP3*, and *MMP9* were significantly increased in the ovary during sexual maturation in chicken. In addition, Hui et al. [29] reported that *MMP3* expression in the GCs decreased significantly during ageing in porcine. In this study, we identified that the expression of MMP3 protein and mRNA were significantly increased in GP-treated GCs in a dose-dependent manner. Kuittinen et al. [56] reported that high *MMP* expression was found in lymphoid and malignant transformed cells. In summary, our results suggested that the upregulation of *MMP3* in GCs is the result of GP cytotoxicity rather than the maturation of the cells.

Survivin (BIRC5) is an inhibitor of apoptosis and has been shown to play an important role in cellular apoptosis by blocking the downstream step of mitochondrial cytochrome c release [57]. Several studies have shown that the BIRC5 protein is an inhibitor of apoptosis and is overexpressed in human cancer cells [58, 59]. Jiang et al. [44] reported that the toxicity of GP was mediated by the expression of genes such as *BIRC5* involved in cell cycle and survival, thereby inhibiting the proliferation of prostate cancer cells. Our mRNA expression results showed that *BIRC5* was downregulated by GP cytotoxicity, indicating that GP induces apoptosis by inhibiting cell proliferation of porcine GCs.

The catalytic reaction of cytochrome P450 proteins (CYPs) is not essential for the maintenance of cellular activity,

but plays an important role in the metabolism and removal of exogenous substances [60]. Enzymes belonging to the CYP family are called phase I enzymes; they monooxygenase, reduce, and hydrolyze various substances such as lipids, steroidal hormones, and xenobiotics [61]. Phase I enzymes are expressed primarily in the liver, but they are also present in other tissues such as uterus, placenta, brain, kidney, and testis [62]. Previous studies have reported that certain CYP isoforms (CYP1A1, CYP1A2 and CYP2B) are present in porcine prepubertal ovary cells [63, 64]. The Ah receptor (AhR) is a transcription factor that mediates the toxic effects of chemicals. Pocar et al. [65] reported that treatment with TCDD (2,3,7,8 tetrachlorodibenzo-p-dioxin) and PCB126 (polychlorinated biphenyl 126) induced the AhR signal transduction response via the expression of *CYP1A1*, an AhR target gene in porcine thyrocyte. In addition, Barć et al. [60] reported that the activity and expression of *CYP1A1* dose-dependently increased in polychlorinated naphthalene-treated porcine GCs. According to the qRT-PCR results in the present study, *CYP1A1* mRNA was significantly increased in GP-treated GCs, which is likely due to GP cytotoxicity. However, RNA-seq results did not show a significant difference in *CYP1A1* mRNA expression with GP treatment, although an upregulation pattern was observed.

The transforming growth factor β (*TGFβ*) gene is involved in several important cellular functions, including proliferation and differentiation. It is also a molecular marker related to embryonic growth and development of mammalian oocytes [66]. Dragovic et al. [67] reported that *TGFβ* gene is an important marker of cumulus expansion, and this process has been shown to be determined by the TGFβ protein signaling pathway. *COL1A*2 is involved in TGFβ signaling, which plays an important role in mediating ovarian age and oocyte quality [68, 69]. The *COL1A2* gene is involved in cellular proliferation and regulation of the cell cycle, and decreased levels of *COL1A2* in old mares indicate the potential deregulation of TGFβ signaling as an underlying factor in the age-related decline in oocyte quality [70]. In the present study, we found that the mRNA expression of the *COL1A2* and *TGFβ3* genes were significantly downregulated. In view of the function of these two genes, these results suggest that GP inhibits the proliferation and differentiation of porcine GCs and thus could affect the growth and development of oocyte.

To evaluate the effect of GP toxicity on intracellular oxidative damage in porcine GCs, the relative mRNA and protein abundance of three genes related to ROS production was analyzed. Peroxiredoxins (PRDXs) are peroxidases that work together to detoxify ROS and provide cytoprotection from internal and external environmental stress [71, 72]. Kubo et al. [73] showed that *PRDXs* are down-regulators of various apoptotic

pathways. In particular, since cumulus-oocyte complexes form a functional entity, the upregulation of PRDX6 in oocytes at the protein level and the accumulation of deadenylated transcripts have been shown to play an important role not only in embryo development but also oocyte maturation [74]. Microsomal glutathione transferase 1 (MGST1) is a member of the membrane-associated proteins in eicosanoid and glutathione metabolism (MAPEG) superfamily [75]. MGST1 is a membrane protein located in the endoplasmic reticulum and the outer mitochondrial membrane that protects cells from oxidative stress [76]. Several studies have reported that MGST1 is activated by a variety of factors, including reactive oxygen ($O2^-$, H_2O_2) and nitrogen ($ONOO^-$, NO) species, sulfhydryl reagents, proteolysis, heating, radiation and dimerization of the homotrimers [77, 78]. In addition, MGST1 has been shown to play an important role in the detoxication of drugs and xenobiotics and may protect membranes against lipid peroxidation [79, 80]. SOD3 is an important antioxidant enzyme located in the ECM of numerous tissues and the glycocalyx of cell surfaces. SOD3 removes superoxide and ROS to prevent cell death and protect normal tissues [81, 82]. In addition, SOD3 may play a critical role in the protection against external environmental factors such as microbiological pathogens [83]. Basina et al. [39] reported that GP stimulates O_2 generation by SOD activity inhibition in porcine GCs. The authors proposed that the increased O_2 levels play a role in reducing steroid production in GCs. In this study, we found that *SOD3* gene was downregulated according to GP concentration. This result is consistent with the SOD activity reported by Basini et al. [39]. Furthermore, in our study, the *MGST1* and *PRDX6* genes were found to be upregulated at both the mRNA and protein levels. Collectively, these results indicate that these genes may be part of the cellular defense against oxidative stress caused by GP toxicity in the differentiation process of GCs.

In conclusion, we used RNA-seq to examine the gene expression profiles of GP-treated porcine GCs. To our knowledge, this is the first time that the effects of GP cytotoxicity in porcine GCs were studied using RNA-seq. We selected a total of 11 genes and classified their functions using GO and KEGG analyses of the DEGs obtained with GP treatment. qRT-PCR and Western blot analysis showed significant differences in the expression of selected genes. However, further studies are warranted to identify the mechanisms underlying the functions of each gene. The results of this study provide a basis for examining the effects of GP toxicity in porcine. In addition, our findings provide greater insight into the various aspects of GP cytotoxicity in GCs.

Supplementary information

Additional file 1 Supplemental Table 1 Primer sequence for qRT-PCR **Supplemental Figure 1** Uncropped Western blot images of Figure 6.

Abbreviations

GP: Gossypol; GCs: Granulosa cells; CM: Cottonseed meal; ROS: Reactive oxygen species; NGS: Next-generation sequencing; RNA-seq: RNA sequencing; PBS: Phosphate-buffered saline; FPKM: Fragments per kilobase of transcripts per million mapped reads; DEGs: Differentially expressed genes; GO: Gene ontology; KEGG: Kyoto encyclopedia of genes and genomes; PVDF: Polyvinylidene fluoride; Ctrl: GP untreated in GCs; GP6.25: GP 6.25 μM treated GCs; GP12.5: GP 12.5 μM treated GCs; IPC: Intersection portion of both concentrations; CPE: Cytoplasmic polyadenylation element; ECM: Extracellular matrix; MMPs: Matrix metalloproteinases; CYPs: Cytochrome P450 proteins

Acknowledgements

We appreciate Yong Hwangbo for sampling porcine ovaries from a local slaughterhouse and transported.

Authors' contributions

M.W.H. conceived and designed the experiments, M.W.H. and H.K. performed animal sampling, M.W.H. and S.Y.C. conducted experiments and wrote manuscript, M.W.H., H.K. and S.Y.C. performed bioinformatics analysis and analyzed the results. S.J.L. supervised the experiments. All authors approved the manuscript.

Funding

This work supported by a grant (No.2017R1A2B2012125) of the National Research Foundation, Republic of Korea.

Availability of data and materials

The datasets used and/or analysed during the current study are available from the corresponding author on request.

Ethics approval

All experimental procedures were conducted in accordance with guidelines approved by the Institutional Animal Care and Use Committee of Kangwon National University, Chuncheon, Korea (KIACUC-18-061).

Consent for publication

Not applicable

Competing interests

The authors declare no competing interests.

References

1. Brocas C, Rivera R, Paula-Lopes F, McDowell L, Calhoun M, Staples C, et al. Deleterious actions of gossypol on bovine spermatozoa, oocytes, and embryos. Biol. Reprod. 1997;57(4):901-907.

2. El-Sharaky A, Newairy A, Elguindy N, Elwafa A. Spermatotoxicity, biochemical changes and histological alteration induced by gossypol in testicular and hepatic tissues of male rats. Food and Chemical Toxicology. 2010;48(12):3354-3361.

3. Coutinho EM. Gossypol: a contraceptive for men. Contraception. 2002;65(4):259-263.

4. Morgan S, Stair E, Martin T, Edwards W, Morgan G. Clinical, clinicopathologic, pathologic, and toxicologic alterations associated with gossypol toxicosis in feeder lambs. Am. J. Vet. Res. 1988;49(4):493-499.

5. Holmberg C, Weaver L, Guterbock W, Genes J, Montgomery P. Pathological and toxicological studies of calves fed a high concentration cotton seed meal diet. Vet. Pathol. 1988;25(2):147-153.

6. Fombad R, Bryant M. An evaluation of the use of cottonseed cake in the diet of growing pigs. Trop. Anim. Health Prod. 2004;36(3):295-305.

7. Fornes M, Barbieri A, Burgos M. Sperm motility loss induced by gossypol: relation with OH. scavengers, motile stimulators and malondialdehyde production. Biochem. Biophys. Res. Commun. 1993;195(3):1289-1293.

8. Kovacic P. Mechanism of drug and toxic actions of gossypol: focus on reactive oxygen species and electron transfer. Curr. Med. Chem. 2003;10(24):2711-2718.

9. Tso W, Lee C. Gossypol uncoupling of respiratory chain and oxidative phosphorylation in ejaculated boar spermatozoa. Contraception. 1982;25(6):649-655.

10. Eppig JJ, Wigglesworth K, Pendola FL. The mammalian oocyte orchestrates the rate of ovarian follicular development. Proc. Natl. Acad. Sci. U. S. A. 2002Mar 5;99(5):2890-2894.

11. Payne AH, Hales DB. Overview of steroidogenic enzymes in the pathway from cholesterol to active steroid hormones. Endocr. Rev. 2004;25(6):947-970.

12. Zhang GL, Zhang RQ, Sun XF, Cheng SF, Wang YF, Ji CL, et al. RNA-seq based gene expression analysis of ovarian granulosa cells exposed to zearalenone in vitro: significance to steroidogenesis. Oncotarget. 2017Jul 31;8(38):64001-64014.

13. Gu Y, Li P, Lin Y, Rikihisa Y, Brueggemeier R. Gossypolone suppresses progesterone synthesis in bovine luteal cells. J. Steroid Biochem. Mol. Biol. 1991;38(6):709-715.

14. Lin Y, Coskun S, Sanbuissho A. Effects of gossypol on in vitro bovine oocyte maturation and steroidogenesis in bovine granulosa cells. Theriogenology. 1994;41(8):1601-1611.

15. Gadelha IC, de Macedo MF, Oloris SC, Melo MM, Soto-Blanco B. Gossypol promotes degeneration of ovarian follicles in rats. ScientificWorldJournal. 2014;2014:986184.

16. Huang W, Khatib H. Comparison of transcriptomic landscapes of bovine embryos using RNA-Seq. BMC Genomics. 2010;11(1):711.

17. Zhao S, Fung-Leung WP, Bittner A, Ngo K, Liu X. Comparison of RNA-Seq and microarray in transcriptome profiling of activated T cells. PLoS One. 2014Jan 16;9(1):e78644.

18. Zhang J, Cheng X, Jin Q, Su X, Li M, Yan C, et al. Comparison of the transcriptomic analysis between two Chinese white pear (Pyrus bretschneideri Rehd.) genotypes of different stone cells contents. PloS one. 2017;12(10):e0187114.

19. Jiang H, Lei R, Ding S, Zhu S. Skewer: a fast and accurate adapter trimmer for next-generation sequencing paired-end reads. BMC Bioinformatics. 2014;15(1):182.

20. Dobin A, Davis CA, Schlesinger F, Drenkow J, Zaleski C, Jha S, et al. STAR: ultrafast universal RNA-seq aligner. Bioinformatics. 2013;29(1):15-21.

21. Trapnell C, Williams BA, Pertea G, Mortazavi A, Kwan G, Van Baren MJ, et al. Transcript assembly and quantification by RNA-Seq reveals unannotated transcripts and isoform switching during cell differentiation. Nat. Biotechnol. 2010;28(5):511.

22. Trapnell C, Hendrickson DG, Sauvageau M, Goff L, Rinn JL, Pachter L. Differential analysis of gene regulation at transcript resolution with RNA-seq. Nat. Biotechnol. 2013;31(1):46.

23. Reimand J, Arak T, Adler P, Kolberg L, Reisberg S, Peterson H, et al. g: Profiler—a web server for functional interpretation of gene lists (2016 update). Nucleic Acids Res. 2016;44(W1):W83-W89.

24. Anders S, Reyes A, Huber W. Detecting differential usage of exons from RNA-seq data. Genome Res. 2012Oct;22(10):2008-2017.

25. Benjamini Y, Hochberg Y. Controlling the false discovery rate: a practical and powerful approach to multiple testing. Journal of the Royal statistical society: series B (Methodological). 1995;57(1):289-300.

26. Schneider CA, Rasband WS, Eliceiri KW. NIH Image to ImageJ: 25 years of image analysis. Nature methods. 2012;9(7):671-675.

27. Croucher NJ, Thomson NR. Studying bacterial transcriptomes using RNA-seq. Curr. Opin. Microbiol. 2010;13(5):619-624.

28. Marioni JC, Mason CE, Mane SM, Stephens M, Gilad Y. RNA-seq: an assessment of technical reproducibility and comparison with gene expression arrays. Genome Res. 2008Sep;18(9):1509-1517.

29. Hui L, Shuangshuang G, Jianning Y, Zhendan S. Systemic analysis of gene expression profiles in porcine granulosa cells during aging. Oncotarget. 2017Oct 10;8(57):96588-96603.

30. Sadowska A, Nynca A, Ruszkowska M, Paukszto L, Myszczynski K, Orlowska K, et al. Transcriptional profiling of porcine granulosa cells exposed to 2, 3, 7, 8-tetrachlorodibenzo-p-dioxin. Chemosphere. 2017;178:368-377.

31. Liu XL, Wu RY, Sun XF, Cheng SF, Zhang RQ, Zhang TY, et al. Mycotoxin zearalenone exposure impairs genomic stability of swine follicular granulosa cells in vitro. Int. J. Biol. Sci. 2018Feb 12;14(3):294-305.

32. Haschek WM, Beasley VR, Buck WB, Finnell JH. Cottonseed meal (gossypol) toxicosis in a swine herd. J. Am. Vet. Med. Assoc. 1989Sep 1;195(5):613-615.

33. Sahin F, Avci CB, Gunduz C, Sezgin C, Simsir IY, Saydam G. Gossypol exerts its cytotoxic effect on HL-60 leukemic cell line via decreasing activity of protein phosphatase 2A and interacting with human telomerase reverse transcriptase activity. Hematology. 2010;15(3):144-150.

34. Volate SR, Kawasaki BT, Hurt EM, Milner JA, Kim YS, White J, et al. Gossypol induces apoptosis by activating p53 in prostate cancer cells and prostate tumor-initiating cells. Mol. Cancer. Ther. 2010Feb;9(2):461-470.

35. Moon D, Choi YH, Moon S, Kim W, Kim G. Gossypol decreases tumor necrosis factor-α-induced intercellular adhesion molecule-1 expression via suppression of NF-κB activity. Food and chemical toxicology. 2011;49(4):999-1005.

36. Atmaca H, Gorumlu G, Karaca B, Degirmenci M, Tunali D, Cirak Y, et al. Combined gossypol and zoledronic acid treatment results in synergistic induction of cell death and regulates angiogenic molecules in ovarian cancer cells. Eur. Cytokine Netw. 2009;20(3):121-130.

37. Konac E, Ekmekci A, Yurtcu E, Ergun MA. An in vitro study of cytotoxic effects of gossypol on human epidermoid larynx carcinoma cell line (HEp-2). Exp Oncol. 2005;27(1):81-83.

38. Badawy SZ, Souid A, Cuenca V, Montalto N, Shue F. Gossypol inhibits proliferation of endometrioma cells in culture. Asian J. Androl. 2007;9(3):388-393.

39. Basini G, Bussolati S, Baioni L, Grasselli F. Gossypol, a polyphenolic aldehyde from cotton plant, interferes with swine granulosa cell function. Domest. Anim. Endocrinol. 2009;37(1):30-36.

40. Hsiao WT, Tsai MD, Jow GM, Tien LT, Lee YJ. Involvement of Smac, p53, and caspase pathways in induction of apoptosis by gossypol in human retinoblastoma cells. Mol. Vis. 2012;18:2033-2042.

41. Gautier J, Minshull J, Lohka M, Glotzer M, Hunt T, Maller JL. Cyclin is a component of maturation-promoting factor from Xenopus. Cell. 1990;60(3):487-494.

42. Murray AW. Creative blocks: cell-cycle checkpoints and feedback controls. Nature. 1992;359(6396):599.

43. Adhikari D, Zheng W, Shen Y, Gorre N, Ning Y, Halet G, et al. Cdk1, but not Cdk2, is the sole Cdk that is essential and sufficient to drive resumption of meiosis in mouse oocytes. Hum. Mol. Genet. 2012;21(11):2476-2484.

44. Jiang J, Slivova V, Jedinak A, Sliva D. Gossypol inhibits growth, invasiveness, and angiogenesis in human prostate cancer cells by modulating NF-κB/AP-1 dependent-and independent-signaling. Clin. Exp. Metastasis. 2012;29(2):165-178.

45. Kuroda T, Naito K, Sugiura K, Yamashita M, Takakura I, Tojo H. Analysis of the roles of cyclin B1 and cyclin B2 in porcine oocyte maturation by inhibiting synthesis with antisense RNA injection. Biol. Reprod. 2004;70(1):154-159.

46. Sugiura K, Naito K, Endo T, Tojo H. Study of germinal vesicle requirement for the normal kinetics of maturation/M-phase-promoting factor activity during porcine oocyte maturation. Biol. Reprod. 2006;74(3):593-600.

47. Stanley JA, Lee J, Nithy TK, Arosh JA, Burghardt RC, Banu SK. Chromium-VI arrests cell cycle and decreases granulosa cell proliferation by down-regulating cyclin-dependent kinases (CDK) and cyclins and up-regulating CDK-inhibitors. Reproductive Toxicology. 2011;32(1):112-123.

48. Mendez R, Richter JD. Translational control by CPEB: a means to the end. Nature reviews Molecular cell biology. 2001;2(7):521.

49. Komrskova P, Susor A, Malik R, Prochazkova B, Liskova L, Supolikova J, et al. Aurora kinase A is not involved in CPEB1 phosphorylation and cyclin B1 mRNA polyadenylation during meiotic maturation of porcine oocytes. PloS one. 2014;9(7):e101222.

50. Stebbins-Boaz B, Cao Q, de Moor CH, Mendez R, Richter JD. Maskin is a CPEB-associated factor that transiently interacts with eIF-4E. Mol. Cell. 1999;4(6):1017-1027.

51. Nakahata S, Kotani T, Mita K, Kawasaki T, Katsu Y, Nagahama Y, et al. Involvement of Xenopus Pumilio in the translational regulation that is specific to cyclin B1 mRNA during oocyte maturation. Mech. Dev. 2003;120(8):865-880.

52. Page-McCaw A, Ewald AJ, Werb Z. Matrix metalloproteinases and the regulation of tissue remodelling. Nature reviews Molecular cell biology. 2007;8(3):221.

53. Curry Jr TE, Osteen KG. Cyclic changes in the matrix metalloproteinase system in the ovary and uterus. Biol. Reprod. 2001;64(5):1285-1296.

54. Smith MF, Ricke WA, Bakke LJ, Dow MP, Smith GW. Ovarian tissue remodeling: role of matrix metalloproteinases and their inhibitors. Mol. Cell. Endocrinol. 2002;191(1):45-56.

55. Zhu G, Kang L, Wei Q, Cui X, Wang S, Chen Y, et al. Expression and regulation of MMP1, MMP3, and MMP9 in the chicken ovary in response to gonadotropins, sex hormones, and TGFB1. Biol. Reprod. 2014;90(3):57, 1-11.

56. Kuittinen O, Apaja-Sarkkinen M, Turpeenniemi-Hujanen T. Gelatinases (MMP-2 and MMP-9), TIMP-1 expression and the extent of neovascularization in aggressive non-Hodgkin's lymphomas. Eur. J. Haematol. 2003;71(2):91-99.

57. Shin S, Sung B, Cho Y, Kim H, Ha N, Hwang J, et al. An anti-apoptotic protein human survivin is a direct inhibitor of caspase-3 and-7. Biochemistry (N. Y.). 2001;40(4):1117-1123.

58. Branca M, Giorgi C, Santini D, Di Bonito L, Ciotti M, Costa S, et al. Survivin as a marker of cervical intraepithelial neoplasia and high-risk human papillomavirus and a predictor of virus clearance and prognosis in cervical cancer. Am. J. Clin. Pathol. 2005;124(1):113-121.

59. Rahman KW, Li Y, Wang Z, Sarkar SH, Sarkar FH. Gene expression profiling revealed survivin as a target of 3,3'-diindolylmethane-induced cell growth inhibition and apoptosis in breast cancer cells. Cancer Res. 2006May 1;66(9):4952-4960.

60. Barć J, Karpeta A, Gregoraszczuk EŁ. Action of Halowax 1051 on Enzymes of Phase I (CYP1A1) and Phase II (SULT1A and COMT) Metabolism in the Pig Ovary
. Int. J. Endocrinol. 2013;2013:590261.

61. Cannady EA, Dyer CA, Christian PJ, Sipes IG, Hoyer PB. Expression and activity of cytochromes P450 2E1, 2A, and 2B in the mouse ovary: the effect of 4-vinylcyclohexene and its diepoxide metabolite. Toxicological Sciences. 2003;73(2):423-430.

62. Xu C, Li CY, Kong AT. Induction of phase I, II and III drug metabolism/transport by xenobiotics. Arch. Pharm. Res. 2005;28(3):249.

63. Ptak A, Ludewig G, Kapiszewska M, Magnowska Z, Lehmler H, Robertson LW, et al. Induction of cytochromes P450, caspase-3 and DNA damage by PCB3 and its hydroxylated metabolites in porcine ovary. Toxicol. Lett. 2006;166(3):200-211.

64. Karpeta A, Warzecha K, Jerzak J, Ptak A, Gregoraszczuk E. Activation of the enzymes of phase I (CYP2B1/2) and phase II (SULT1A and COMT) metabolism by 2, 2′, 4, 4′-tetrabromodiphenyl ether (BDE47) in the pig ovary. Reproductive Toxicology. 2012;34(3):436-442.

65. Pocar P, Klonisch T, Brandsch C, Eder K, Frohlich C, Hoang-Vu C, et al. AhR-agonist-induced transcriptional changes of genes involved in thyroid function in primary porcine thyrocytes. Toxicological sciences. 2006;89(2):408-414.

66. Jackowska M, Kempisty B, Woźna M, Piotrowska H, Antosik P, Zawierucha P, et al. Differential expression of GDF9, TGFB1, TGFB2 and TGFB3 in porcine oocytes isolated from follicles of different size before and after culture in vitro. Acta Vet. Hung. 2013;61(1):99-115.

67. Dragovic RA, Ritter LJ, Schulz SJ, Amato F, Thompson JG, Armstrong DT, et al. Oocyte-secreted factor activation of SMAD 2/3 signaling enables initiation of mouse cumulus cell expansion. Biol. Reprod. 2007;76(5):848-857.

68. Fair T. Mammalian oocyte development: checkpoints for competence. Reproduction, Fertility and Development. 2009;22(1):13-20.

69. Luo S, Kleemann GA, Ashraf JM, Shaw WM, Murphy CT. TGF-β and insulin signaling regulate reproductive aging via oocyte and germline quality maintenance. Cell. 2010;143(2):299-312.

70. da Silveira JC, Winger QA, Bouma GJ, Carnevale EM. Effects of age on follicular fluid exosomal microRNAs and granulosa cell transforming growth factor-β signalling during follicle development in the mare. Reproduction, Fertility and Development. 2015;27(6):897-905.

71. Verdoucq L, Vignols F, Jacquot JP, Chartier Y, Meyer Y. In vivo characterization of a thioredoxin h target protein defines a new peroxiredoxin family. J. Biol. Chem. 1999Jul 9;274(28):19714-19722.

72. Wood ZA, Schröder E, Harris JR, Poole LB. Structure, mechanism and regulation of peroxiredoxins. Trends Biochem. Sci. 2003;28(1):32-40.

73. Kubo E, Singh DP, Fatma N, Akagi Y. TAT-mediated peroxiredoxin 5 and 6 protein transduction protects against high-glucose-induced cytotoxicity in retinal pericytes. Life Sci. 2009;84(23-24):857-864.

74. Leyens G, Verhaeghe B, Landtmeters M, Marchandise J, Knoops B, Donnay I. Peroxiredoxin 6 is upregulated in bovine oocytes and cumulus cells during in vitro maturation: role of intercellular communication. Biol. Reprod. 2004;71(5):1646-1651.

75. Jakobsson P, Morgenstern R, Mancini J, Ford-Hutchinson A, Persson B. Common structural features of MAPEG—a widespread superfamily of membrane associated proteins with highly divergent functions in eicosanoid and glutathione metabolism. Protein Science. 1999;8(3):689-692.

76. Hetland TE, Nymoen DA, Emilsen E, Kærn J, Tropé CG, Flørenes VA, et al. MGST1 expression in serous ovarian carcinoma differs at various anatomic sites, but is unrelated to chemoresistance or survival. Gynecol. Oncol. 2012;126(3):460-465.

77. Imaizumi N, Miyagi S, Aniya Y. Reactive nitrogen species derived activation of rat liver microsomal glutathione S-transferase. Life Sci. 2006;78(26):2998-3006.

78. Ji Y, Neverova I, Van Eyk JE, Bennett BM. Nitration of tyrosine 92 mediates the activation of rat microsomal glutathione s-transferase by peroxynitrite. J. Biol. Chem. 2006Jan 27;281(4):1986-1991.

79. Johansson K, Åhlen K, Rinaldi R, Sahlander K, Siritantikorn A, Morgenstern R. Microsomal glutathione transferase 1 in anticancer drug resistance. Carcinogenesis. 2007;28(2):465-470.

80. Siritantikorn A, Johansson K, Åhlen K, Rinaldi R, Suthiphongchai T, Wilairat P, et al. Protection of cells from oxidative stress by microsomal glutathione transferase 1. Biochem. Biophys. Res. Commun. 2007;355(2):592-596.

81. Marklund SL. Extracellular superoxide dismutase and other superoxide dismutase isoenzymes in tissues from nine mammalian species. Biochem. J. 1984Sep 15;222(3):649-655.

82. Sandstrom J, Karlsson K, Edlund T, Marklund SL. Heparin-affinity patterns and composition of extracellular superoxide dismutase in human plasma and tissues. Biochem. J. 1993Sep 15;294 (Pt 3)(Pt 3):853-857.

83. Kwon M, Lee K, Lee H, Kim J, Kim T. SOD3 variant, R213G, altered SOD3 function, leading to ROS-mediated inflammation and damage in multiple organs of premature aging mice. Antioxidants & redox signaling. 2015;23(12):985-999.

Figures

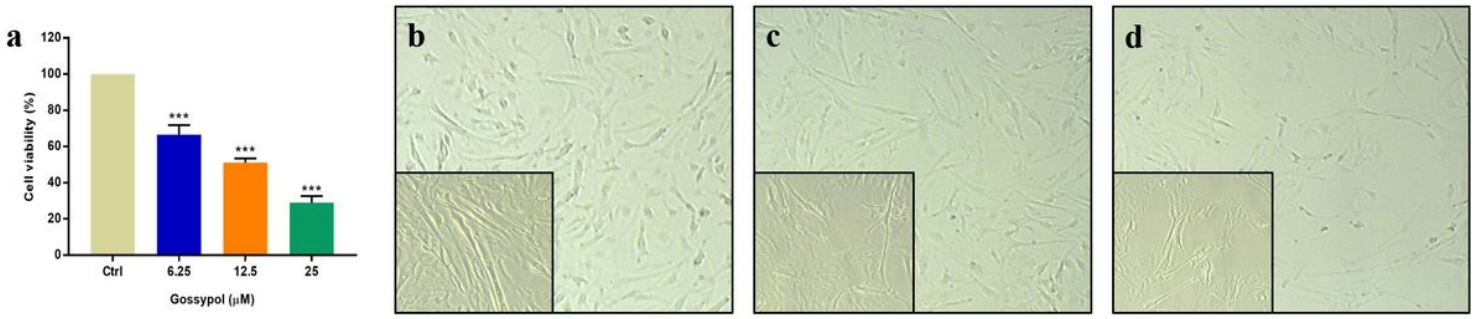

Figure 1

Effect of GP on the viability of porcine GCs in vitro. Porcine GCs were cultured with 0, 6.25, 12.5 and 25 μM GP for 72 h. (a) GC viability at different concentrations (6.25–25 μM) of GP. Data are expressed as mean ± SEM (n = 3) ***p < 0.001. (b)–(d) present the morphology of cultured GCs treated with GP. Large pictures were captured at 40× magnification, while small pictures were captured at 100× magnification. (b) GCs cultured in 0 μM GP (non-treated). (c) GCs cultured in 6.25 μM GP. (d) GCs cultured in 12.5 μM GP. GP: gossypol, GCs: granulosa cells, Ctrl: GP untreated in GCs.

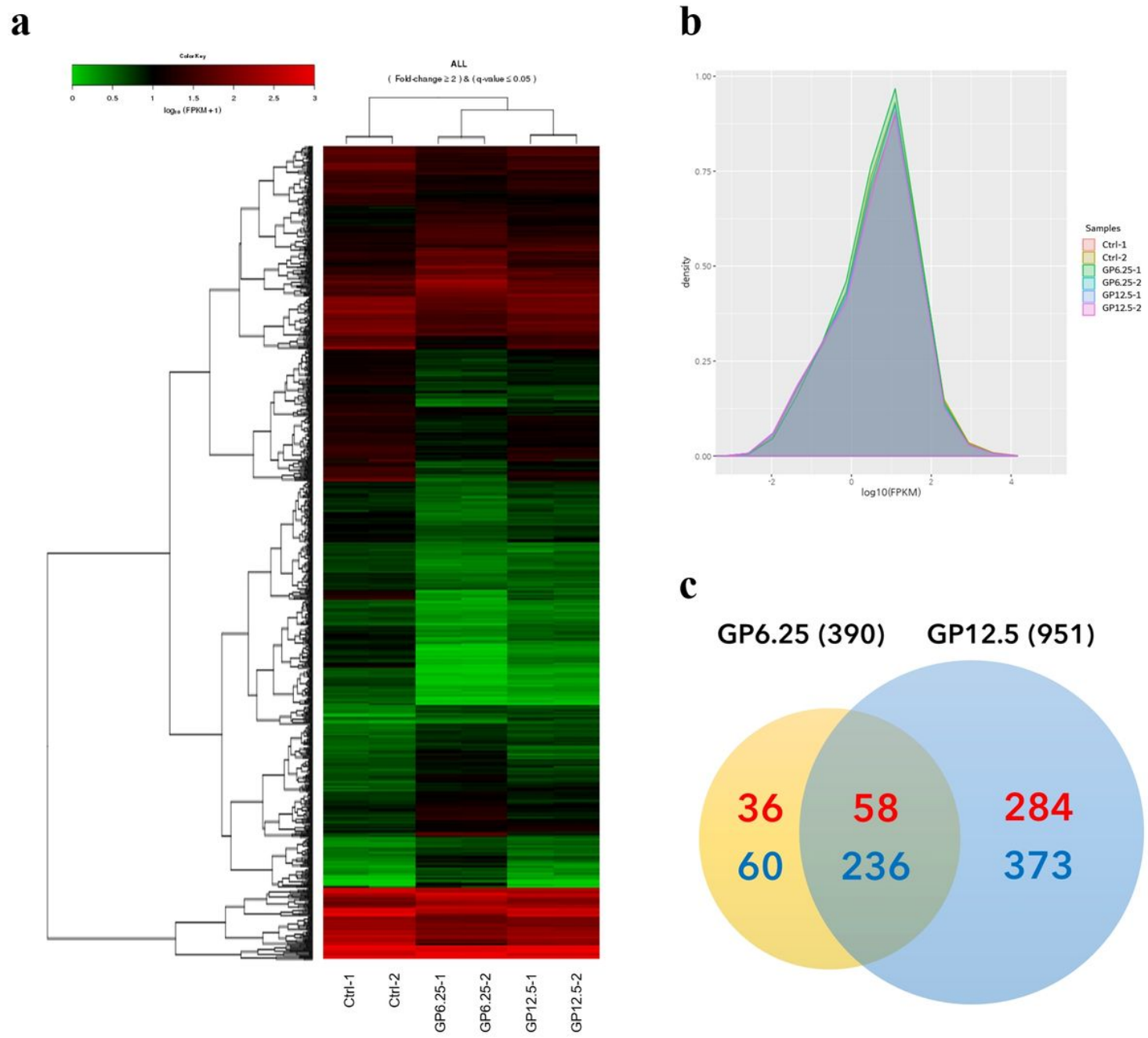

Figure 2

Summary of RNA-seq mapping data. (a) Comparative expression of selected transcriptomes across the GP-treated and Ctrl groups. Heatmap for the expression values in log10 (FPKM) units of the selected DEGs. Red indicates upregulated, while green indicated downregulated gene expression ($p < 0.05$). (b) Density plot for log10 (FPKM) values to compare gene expression between each sample. (c) Venn diagram showing the number of differently expressed genes between the GP6.25 and GP12.5 groups ($p < 0.05$). Red colour: upregulated, Blue colour: downregulated, Ctrl: GP untreated GCs, GP6.25: GP 6.25 μM treated GCs, GP12.5: GP 12.5 μM treated GCs, GP: gossypol, GCs: granulosa cells

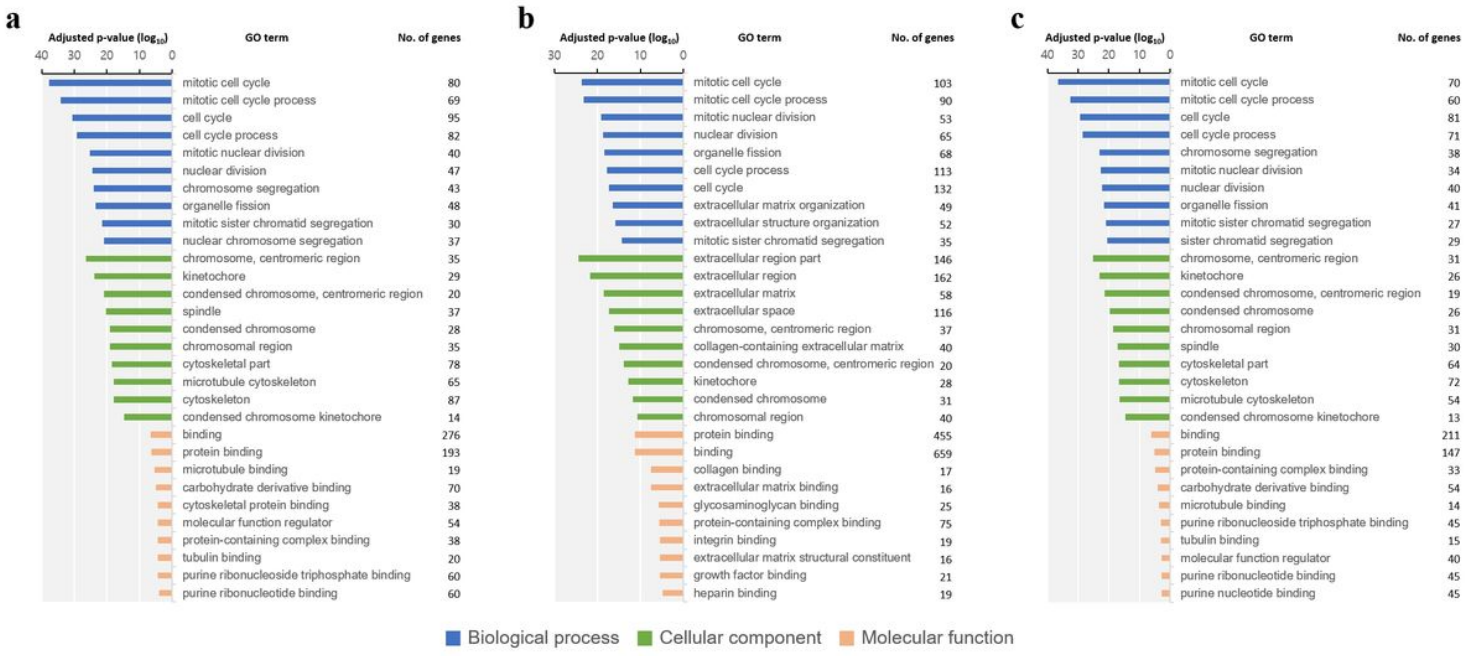

Figure 3

GO functional analysis of DEGs. GO term enrichment analysis results based on the different GP treatments were retrieved and compared with the Ctrl group using g:Profiler (https://biit.cs.ut.ee/gprofiler). The 10 most significantly ($p < 0.05$) enriched GO terms related to biological processes, cellular components and molecular functions are sown. All adjusted statistically significant values of the terms were −log10 converted. (a) GO term enrichment result of the DEGs in the GP6.25 group. (b) GO term enrichment result of the DEGs in the GP12.5 group. (c) GO term enrichment result of the DEGs in IPC group. GO: gene ontology, GP: gossypol, Ctrl: GP untreated GCs, GP6.25: GP 6.25 μM treated GCs, GP12.5: GP 12.5 μM treated GCs, IPC: intersection portion of both concentrations, GO: gene ontology, DEGs: differentially expressed genes

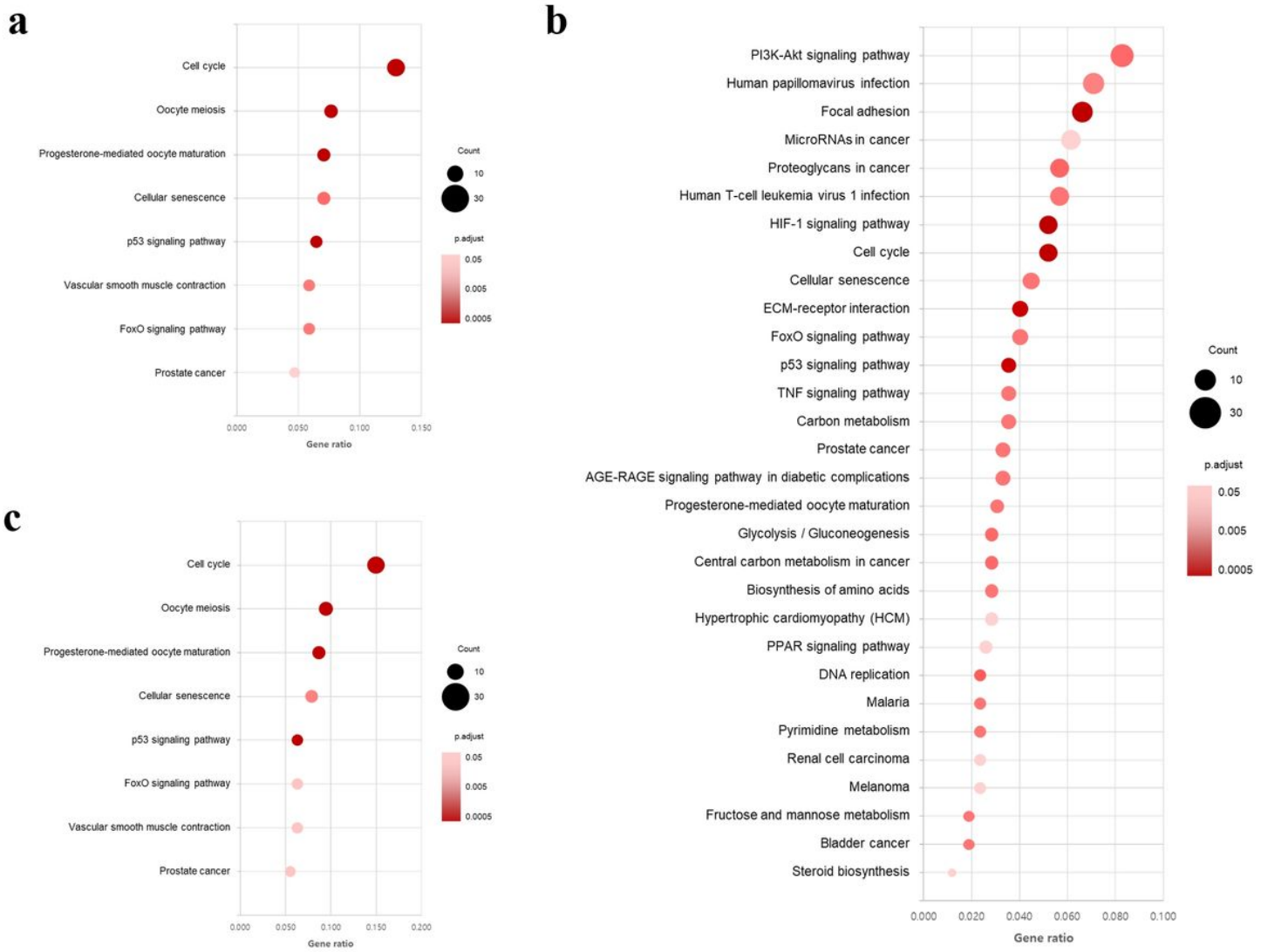

Figure 4

A scatter plot of the significantly enriched KEGG pathways ($p < 0.05$, www.kegg.jp/kegg/kegg1.html) of the DEGs based on transcriptome sequencing analysis of each GP-treated group compared with the Ctrl group. The y-axis represents the name of the pathway, while the x-axis represents the gene ratio. Dot size represents the number of genes and the colour indicated the p-value. (a) Enriched KEGG pathways of the DEGs in the GP6.25 group. (b) Enriched KEGG pathways of the DEGs in the GP12.5 group. (c) Enriched KEGG pathways of the DEGs in the IPC group. KEGG: Kyoto encyclopaedia of genes and genomes, DEGs: differentially expressed genes, GP6.25: GP 6.25 μM treated GCs, GP12.5: GP 12.5 μM treated GCs, IPC: intersection portion of both concentrations

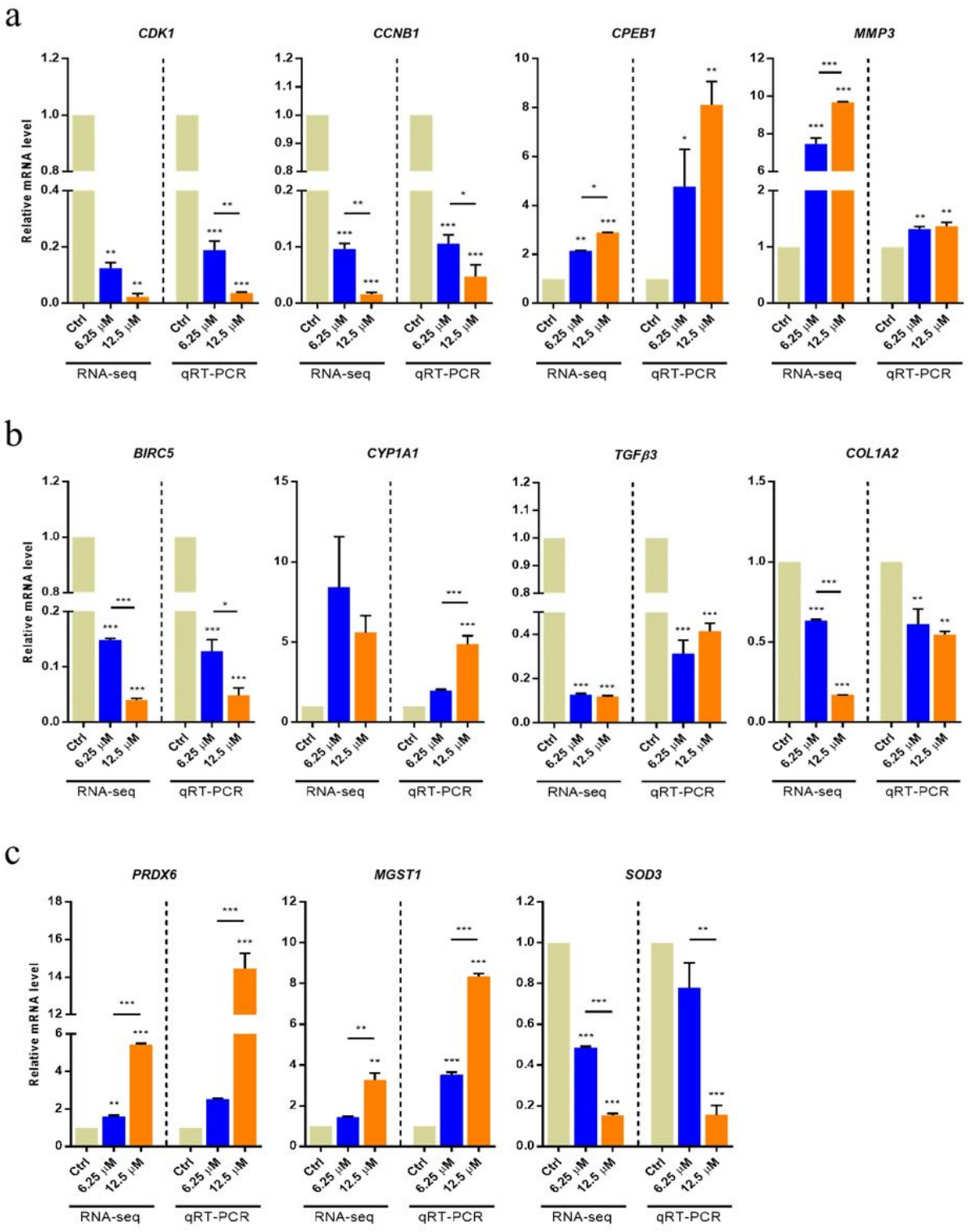

Figure 5

Quantification of the mRNA profile of GP-treated GCs (6.25 and 12.5 μM) using RNA-seq and qRT-PCR. GCs incubated with each GP concentration for 72 h. GP exposure affected the mRNA abundance of certain genes in the cells. (a) Cellular component organisation related genes (BIRC5, CYP1A1, COL1A2 and TGFβ3) were measured and presented. (b) The female reproductive functions related genes (CDK1, CCNB1, CPEB1 and MMP3) measured and presented. (c) Oxidation-reduction process related genes

(PRDX6, MGST1 and SOD3) were measured and presented. The mRNA levels of all genes were normalised to the porcine β-actin gene. Results are presented as mean ± SEM. All experiments were repeated at least three times. Ctrl: GP untreated GCs, GP: gossypol, GCs: granulosa cells, *p < 0.05; **p < 0.01; ***p < 0.001.

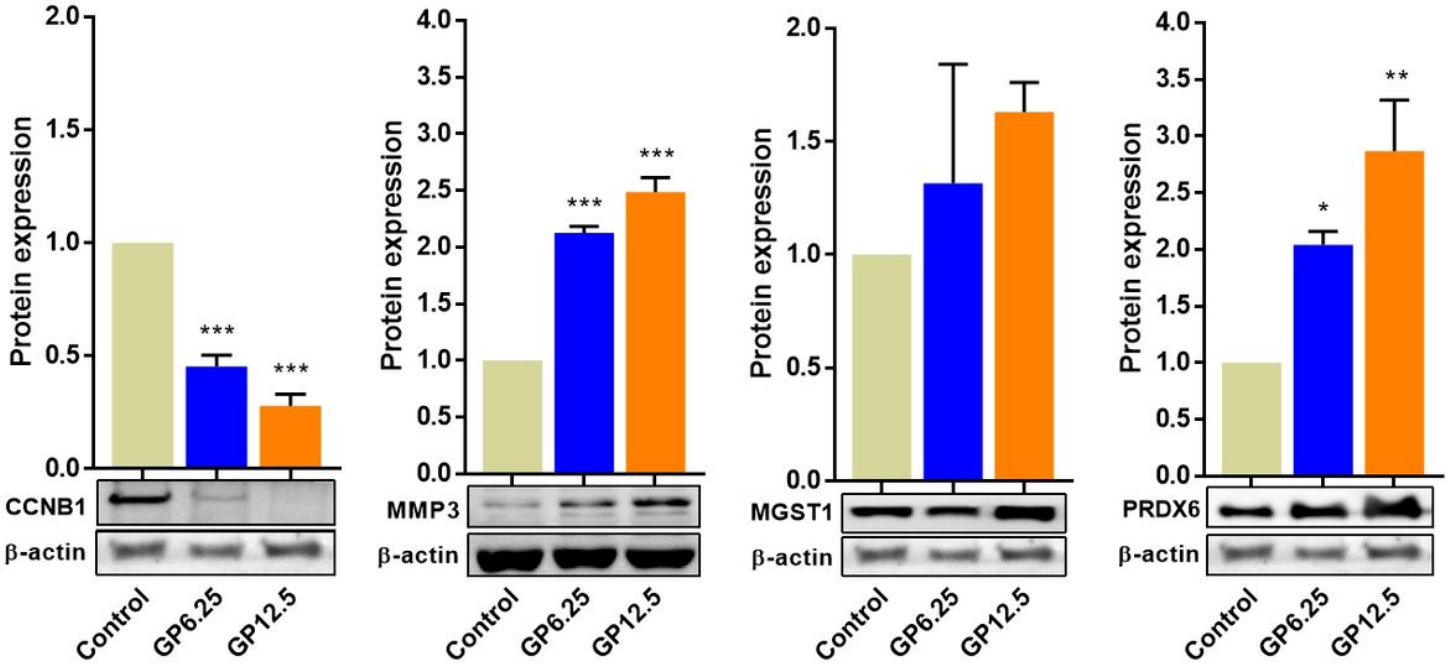

Figure 6

Western blot analysis of CCNB1, MMP3, MGST1 and PRDX6 proteins with different concentration of GP (6.25 and 12.5 μM) in porcine GCs. The protein levels were normalised to β-actin. Data are expressed as the mean ± SEM. All experiments were repeated at least three times. Full-length images for above cropped images are presented in Supplementary Fig. 1. Ctrl: GP untreated GCs, GP: gossypol, GCs: granulosa cells, *: p < 0.05, **: p < 0.01, ***: p < 0.001

Supplementary Files

This is a list of supplementary files associated with this preprint. Click to download.

- 210211Additionalfile.pdf